

# EXPERIMENTS IN NUMERICAL OBJECTIVE FRONTAL ANALYSIS<sup>1</sup>

ROBERT J. RENARD<sup>2</sup>

U.S. Naval Postgraduate School, Monterey, Calif.

and

LEO C. CLARKE

U.S. Navy Fleet Numerical Weather Facility, Monterey, Calif.

## ABSTRACT

A major area of weather analysis still requiring manual subjective determination is that of locating fronts. The experiments reported on here concern an attempt to incorporate objective frontal analysis into the operational computer routines of the U.S. Navy Fleet Numerical Weather Facility, Monterey, Calif.

The synoptically-important numerically-derived frontal zone is regarded as a hyperbaroclinic region whose boundaries may be defined as quasi first-order thermal and moisture discontinuities; the boundaries are located through use of suitably defined second derivatives of various potential temperature parameters. Application is made to 850-mb. and surface (or 1000-mb.) frontal analyses on a hemispheric basis. The analyses for 0000 and 1200 GMT January 1, 1965 are selected to exemplify results of the most promising of the experiments.

Verification against hand-derived frontal analyses, difficulties with the existing scheme, and proposed modifications to the continuing program are discussed.

## 1. INTRODUCTION

It should come as no surprise that the "state of the art" in frontal analysis is still very much dependent on the individual and hence inexact. One illustration will suffice as evidence of the degree of subjective variability. Figure 1 represents the composite of 0000 GMT March 5, 1964 surface fronts as drawn by 16 international and United States civilian and military analysis and forecast centers. It is rather disturbing to see such large differences in frontal positions—in many areas over 300 n. mi.—and to think that such gross misplacements could figure significantly in decision making involving the national economy. March 5, 1964 is not a singularly bad day! A logical solution to this ever-present dilemma is accurate, standardized, objective frontal analysis.

Up to a few years ago objective frontal analysis could, at best, be based on subjectively analyzed input parameters. However, the time has come when fields of data containing frontal information are numerically produced in such a manner as to lend themselves to an objective frontal analysis. Such experiments are reported on here as performed with and on objectively calculated fields of data at the U.S. Navy Fleet Numerical Weather Facility (FNWF), Monterey, Calif.

## 2. DEFINITION OF FRONT AND SELECTION OF FRONTAL PARAMETERS

The definition of a front adopted here is similar to that suggested by the Southern Hemisphere meteorologists, Taljaard, Schmitt, and van Loon [1], in their exhaustive résumé of frontal analysis.

The words *front* or *numerical front*, as used hereafter, refer to the warm-air boundary of a synoptic-scale baroclinic zone of distinct thermal gradient; the frontal zone separates air masses associated with reduced baroclinicity over a considerable area. Further, the frontal-zone boundaries are considered as quasi first-order thermal and moisture discontinuities. Moreover, the hyperbaroclinic regions [2] of interest should be trackable in time and have space continuity through enough of the lower atmosphere to manifest themselves not only at the surface but at 850 mb. as well.

From the outset the aim has been to select a *minimum* number of conservative parameters for specifying the frontal zones while at the same time utilizing the full capacity of FNWF's output, with a view toward producing a result operationally usable in real time. These are stringent demands.

In considering the selection of suitable frontal parameters, thought was given to the frontal information desired by the field meteorologist. An all-inclusive numerical product should

<sup>1</sup> Modified version of paper presented January 27, 1965 at the 45th Annual American Meteorological Society Meeting in New York City.

<sup>2</sup> Research supported by U.S. Navy Fleet Numerical Weather Facility, Monterey, Calif., and the Office of Naval Research.

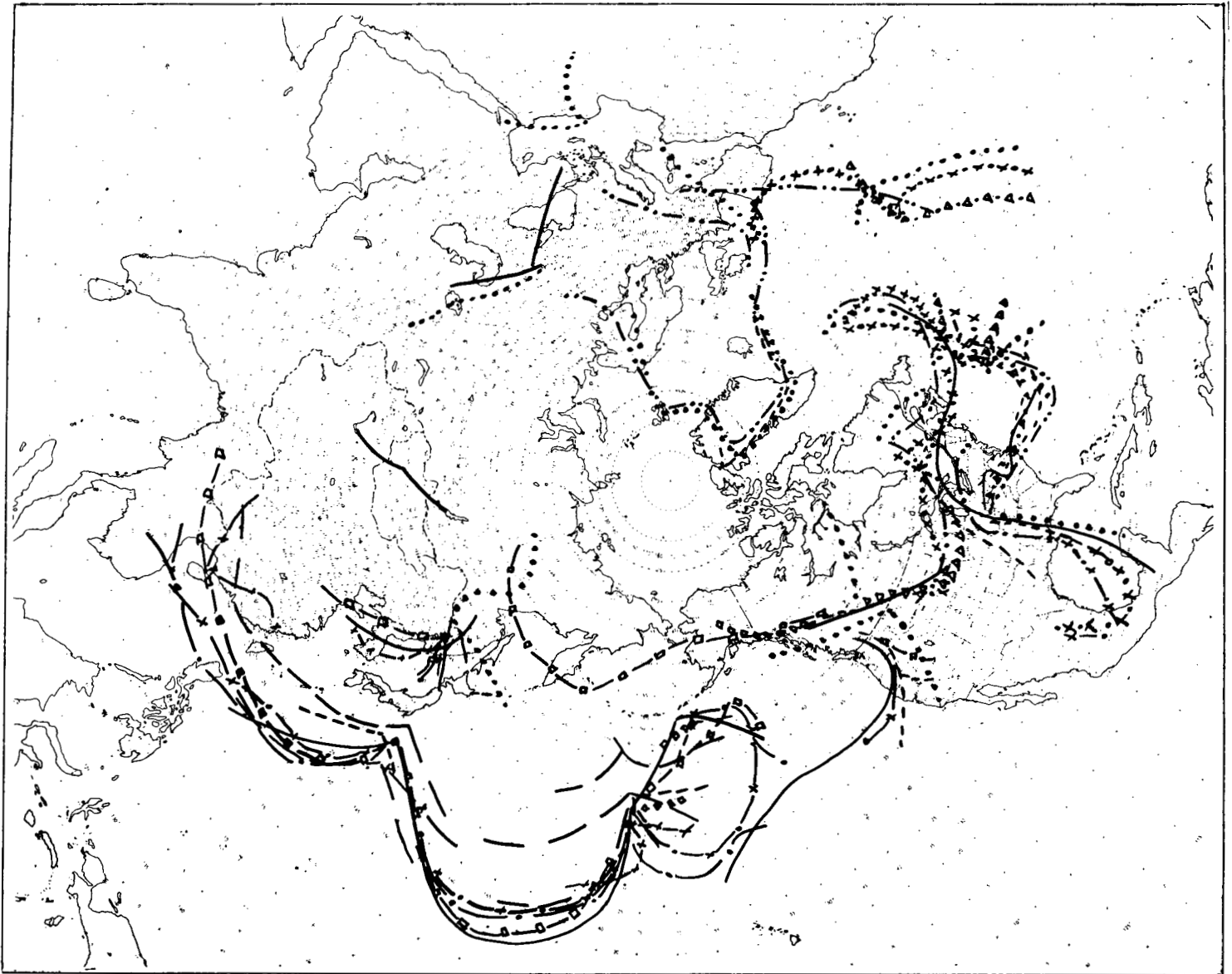


FIGURE 1.—Surface fronts for 0000 GMT March 5, 1964 as taken from analyses made by 16 international and national weather centers. International weather centers: National Meteorological Center, U.S. Weather Bureau; Central Analysis Office, Meteorological Branch, Department of Transport, Canada; Japanese Meteorological Agency; British Meteorological Office; Zentralamt, Deutscher Wetterdienst; Icelandic Weather Bureau. U.S. Navy Weather Centrals: Alameda, Calif.; Guam; Pearl Harbor, Hawaii. U.S. Navy Weather Facilities: Argentia, Newfoundland; Miami; Norfolk, Va.; Quonset Point, R.I.; San Diego; Sangley Point, Philippine Islands; and Yokosuka, Japan.

- a. locate the warm-air boundary of each synoptic-scale baroclinic zone at one or more levels;
- b. attach a "strength" label to every segment of a front;
- c. distinguish fronts according to movement: warm, cold, stationary;
- d. determine the frontolytical/frontogenetical character of the fronts;
- e. relate the frontal-zone slope and stage of development to vertical motion, clouds, precipitation, and development of pressure systems; and
- f. identify the air masses separated by the fronts.

With due regard for the theoretical, operational, and numerical aspects of frontal analysis, the wet-bulb potential temperature ( $\theta_w$ ), equivalent potential temperature ( $\theta_e$ ), potential temperature ( $\theta$ ), and their derivatives were initially selected, collectively, as prime parameters to specify the location of fronts. The wind field was reserved for a secondary role, hydrometeors for a last consideration.

### 3. NUMERICAL INPUT DATA AND ANALYSIS

The data used as input in the experiments are those

objectively analyzed by FNWF from worldwide coverage of more than 2,500 surface reports and 500 raobs. These data are processed at 12-hr. intervals to produce objective analyses of sea level pressure, height, and temperature for all mandatory pressure surfaces up to 200 mb., and dew point depression at terrain level, 850, 700, and 500 mb.

Except for terrain-level parameters the above analyses are produced on a square grid, 63 x 63, wherein the equator is an inscribed circle. The mesh length is 381 km. at 60° latitude on a Northern Hemisphere polar stereographic projection.

The upper-air information is processed in a scheme in which the mandatory-level data of the transmitted soundings are analyzed to fit a five-layered atmosphere in which temperature is linear in  $p^k$  (where  $p$  is pressure;  $k = R_d/c_p$ ;  $R_d$  is the gas constant; and  $c_p$  is the specific heat constant for dry air). The lapse rate (or stability) of each layer is initially specified to be consistent with the actual thickness. The objective constant pressure analyses are in hydrostatic agreement in the vertical and compatible in the horizontal. The fields of temperature and moisture so produced are adequate for computation of the desired potential temperature parameters. Other details of the mass-structure model used by FNWF may be obtained from [3].

The determination of  $\theta_w$ ,  $\theta_e$ , or  $\theta$  at the surface or terrain level is more complex, since the station or terrain pressure for land areas is not available from the surface synoptic reports. To remedy this, terrain pressure and temperature are interpolated from the analyzed upper-air data and the height of the terrain on an octagonally-bounded grid of 1,977 points.

The finite difference approximations to the temperature derivatives utilize the quartic interpolation polynomials for centered differences, in the form

$$\Delta_x(\ ) \text{ at } i=0 = \frac{1}{12d} \left\{ (\ )_{i-2} + 8[(\ )_{i+1} - (\ )_{i-1}] - (\ )_{i+2} \right\} \quad (1)$$

where  $d$  = mesh length. The first derivatives were processed with a low pass filter, having a cut-off wavelength of four mesh lengths, before further differentiation

#### 4. NATURE OF EXPERIMENT

Initial experimentation with fields of potential temperature parameters and their derivatives was carried out on a hemispheric basis at 850 mb. rather than at terrain or sea level. Several reasons suggested this approach, not the least of which is the distinctiveness of fronts (especially polar) at 850 mb. and the apparent lack of mesoscale noise so evident in the surface data.

Moreover, our first attempts at frontal analysis were somewhat idealistic and involved first  $\theta_w$ , then  $\theta_e$ . We were initially influenced by the Canadian school of thought, as described by Godson [2] and Anderson, Boville,

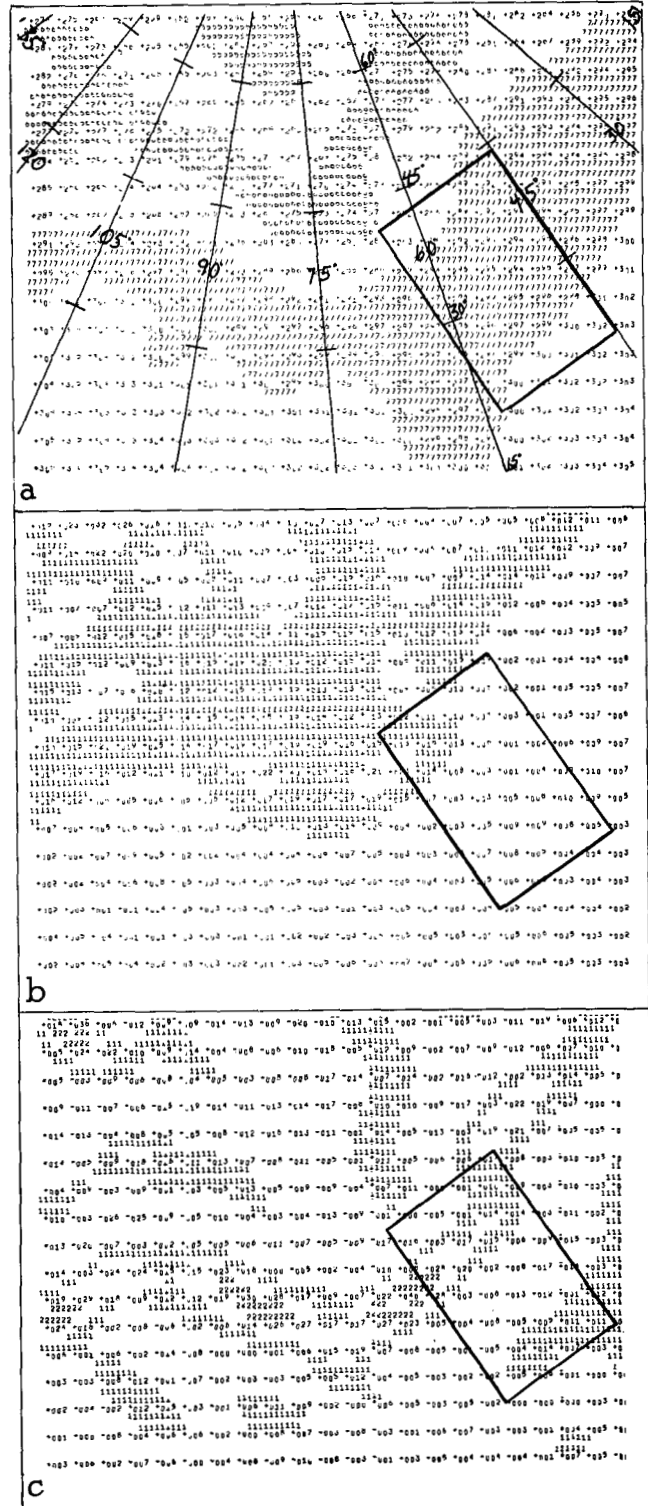


FIGURE 2.—Computer printouts for 850 mb., 0000 GMT January 1, 1965. (a) Grid point values of  $\theta$  in °C. Dummy-number shading at interval of 10°. Skeleton latitude-longitude grid identifies area. (b) Grid point values of  $|\nabla\theta|$  in units of 10<sup>-1</sup>°C./ (100 km.). Dummy-number shading at interval of 10 units starting with 10. (c) Grid point values of  $GG\theta$  in units of 10<sup>-2</sup>°C./ (100 km.)<sup>2</sup>. Dummy-number shading in positive  $GG\theta$  areas only at interval of 10 units starting with 5. Outlined rectangular area is expanded in figure 3.

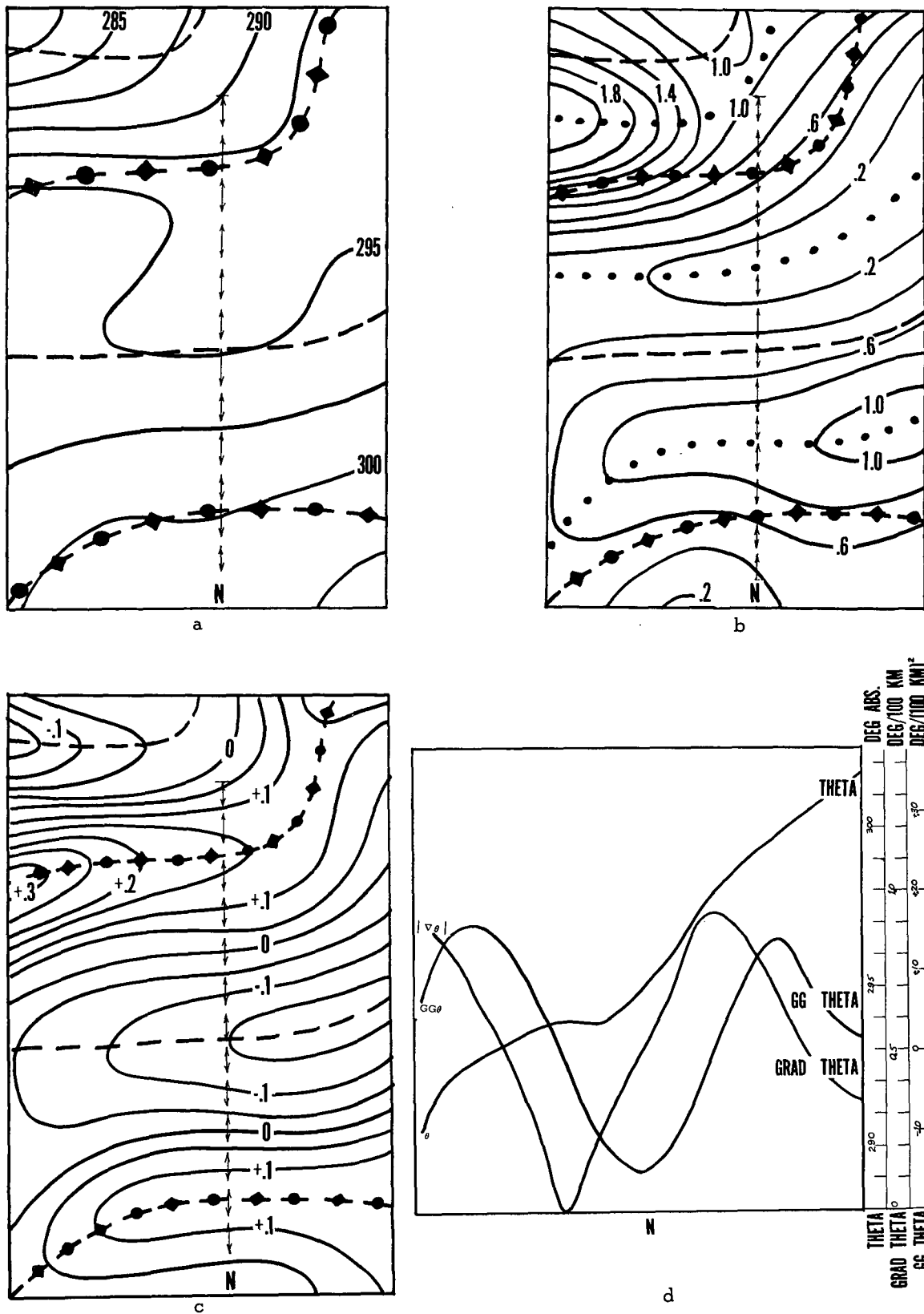


FIGURE 3.—(a) Field of  $\theta$  ( $^{\circ}\text{A}$ .) and derived frontal parameters for the rectangular North Atlantic area shown in figure 2. Troughs in  $GG\theta$  field are shown by dashed lines, ridges by dashed lines with superposed symbols. (b)  $|\nabla\theta|$  in  $^{\circ}\text{C}/(100\text{ km})$  and derived frontal parameters as calculated from figure 3a. Ridges and troughs in  $|\nabla\theta|$  field shown by dotted line. Other lines as in 3a. (c) Field of  $GG\theta = -(\nabla|\nabla(\theta)| \cdot \nabla\theta)/|\nabla\theta|$  in  $^{\circ}\text{C}/(100\text{ km})^2$  as calculated from figure 3a. Other lines as in 3a. (d) Cross-sectional view of  $\theta$ ,  $|\nabla\theta|$ , and  $GG\theta$  taken along line N in figures 3 a, b, c.

and McClellan [4] and others in the 1950's, and given additional impetus by statistics on characteristic air-mass values for  $\theta_w$  by Harley [5] in 1962. However, certain deficiencies in adequately depicting hemispheric moisture fields resulted in the shift of experimental emphasis to fields of  $\theta$  and its derivatives. Unless said otherwise, the following discussion refers to  $\theta$  fields only.

## 5. NUMERICAL FRONTAL PARAMETER AND ITS SIGNIFICANCE

The frontal parameter finally selected is simple, easily computed, and its application to locate a front simulates in an objective manner the procedure followed by a synoptic meteorologist. Specifically, the parameter is defined as *the directional derivative of the gradient of  $\theta$  along its gradient*, namely

$$GG\theta = -\frac{\nabla|\nabla\theta| \cdot \nabla\theta}{|\nabla\theta|} \equiv -\nabla|\nabla\theta| \cdot n_\theta \quad (2)$$

where  $n_\theta$  is a unit vector in the direction of  $\nabla\theta$ .

Actual FNWF computer printouts of a limited section of the objectively analyzed fields of  $\theta$ ,  $|\nabla\theta|$ , and  $GG\theta$  at 850 mb., 0000 GMT January 1, 1965 are shown in figure 2. These printouts will be referred to later.

To obtain an understanding of the properties and uses of a  $GG\theta$  field, a small section of figures 2 a, b, and c is enlarged and analyzed to become figures 3 a, b, c.

Figure 3a shows a subjective analysis of the numerically computed field of  $\theta$ ; the isentropic field obviously contains two zones of marked gradient. Figures 3 b and c show the derived fields of  $|\nabla\theta|$  and  $GG\theta$ . It is to be noted that the axes of maximum and minimum  $|\nabla\theta|$  in figure 3b nearly coincide with zero  $GG\theta$  in figure 3c.<sup>3</sup> The axis of maximum  $|\nabla\theta|$  defines the centrum of the baroclinic zone while the axis of minimum  $|\nabla\theta|$  locates the centrum of the "barotropic" region.

The locus of points along which  $|\nabla\theta|$  changes most rapidly in the direction of  $n_\theta$  defines the *ridge* (*maximum  $GG\theta$* ) and *trough* (*minimum  $GG\theta$* ) in the  $GG\theta$  field. In turn, the *ridge* and *trough* locate the *warm* and *cold* air boundaries of the frontal zone, respectively. The axes of maximum and minimum  $GG\theta$  are superimposed on figures 3 a, b, c.

The transverse width of the frontal zone (distance from maximum to minimum in the  $GG\theta$  field) and maximum magnitude of  $|\nabla\theta|$  within the zone may be used singly or in combination as indicators of the strength of each segment of the front. The apparently high correlation existing between maximum  $|\nabla\theta|$  in the zone and maximum  $GG\theta$  at the adjacent frontal boundary also allows use of the latter as a strength indicator.

A cross-sectional view of the three fields of  $\theta$ ,  $|\nabla\theta|$ , and  $GG\theta$  (fig. 3d) taken along N in figures 3 a, b, and c confirms the relationships existing among the various analyses and allows a point by point comparison of the three fields.

<sup>3</sup> Imperfect coincidence here and in figure 3d is likely as a result of finite difference approximations to the analytic expressions.

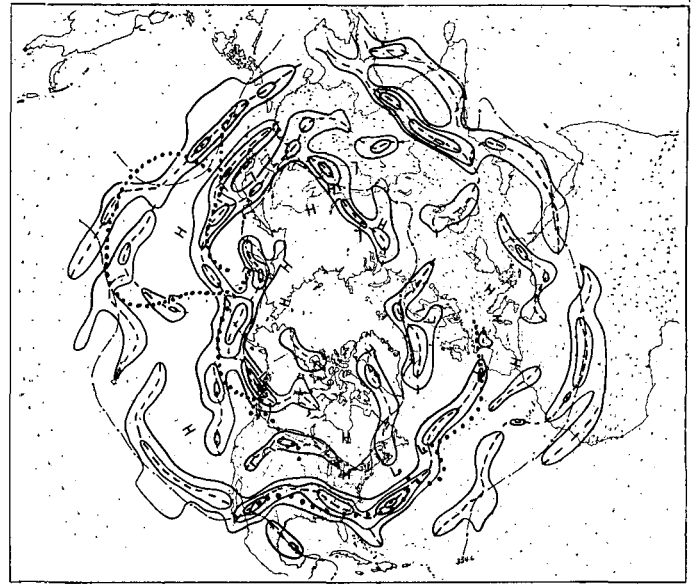


FIGURE 4.— $GG\theta$  (solid lines) analysis at 850 mb. for 0000 GMT January 1, 1965; units  $10^{-2} \text{C.}/(100 \text{ km.})^2$ ; isolines 5, 15, 25, etc. For explanation see text, section 6.

It is to be noted that, more generally, equation (2) may be written as an operator

$$GG(\zeta) = -\nabla|\nabla(\zeta)| \cdot n_{(\zeta)} \quad (3)$$

which is applicable to any variable ( $\zeta$ ) with defined first and second derivatives. It follows that the mathematical and physical significance of  $GG\theta$ , just discussed, is pertinent to the more universal application of the  $GG$  operator.

## 6. DISCUSSION OF FRONTAL-ANALYSIS ILLUSTRATIONS

The analyses for 0000 and 1200 GMT, January 1, 1965 have been selected to illustrate the numerical experiment in frontal analysis. The two map times highlight both the merits and deficiencies of the present state of the technique.

Analyses of the various fields, as discussed hereafter, were traced by hand from FNWF numerical printouts to 1/30,000,000 polar stereographic base maps. In this way attention may be focused upon the major features supporting an objective frontal analysis and not on extraneous features or the maze of numbers and peculiarities of contouring found on computer printouts (fig. 2). The FNWF automated line-drawers are being programed to accomplish the complete analysis task on a real-time basis; however, portrayal for the user is not our concern here.

Figure 4 is the 850-mb.  $GG\theta$  chart for 0000 GMT January 1, 1965. This figure and figures 6 and 8 show certain notable lines and points, whose legend is explained below:

a. The isolines of *positive  $GG\theta$  only* are shown (solid lines). The analysis interval is  $0.1 \text{C.}/(100 \text{ km.})^2$ , starting

with the 0.05 isopleth. With reference to section 5 and figures 3 c and d, the positive  $GG\theta$  values are found in the area between the maximum and minimum potential temperature gradient on the warm-air side of the former.

b. The  $GG\theta$  ridge or line of maximum  $GG\theta$  (dashed) represents the numerical 850-mb. front. Assuming symmetry of the frontal zone about the maximum gradient, the area between the ridge and the 0.05 line toward the cold air represents an approximation to the warmest half of the hyperbaroclinic zone.<sup>4</sup> In the real atmosphere this area is generally less than one-half the area of the frontal zone.

c. The dotted line indicates the *surface* fronts for the same time, as taken from the final analysis of the Northern Hemisphere surface chart of the National Meteorological Center, U.S. Weather Bureau (USWB). The surface Highs (H) and Lows (L) are positions taken from the same analysis. The USWB's 850-mb. pressure center and frontal analyses were not used for this comparison since the area for which they are available is too limited.

d. Harley [5] defines, statistically, mean and standard deviations of  $\theta_w$  for each of four prominent air masses (maritime tropical, maritime polar, maritime Arctic, and continental Arctic). If the air masses are taken as quasi-barotropic, the statistics may be interpreted to be broadly representative of mean frontal values. Values for January follow (Harley's  $\bar{\theta}_w$  values have been converted to  $\bar{\theta}_e$ ):

Front	$\bar{\theta}_e$ (°A.)	Air mass
polar (p)	315.3	tropical
maritime (m)	303.4	maritime polar
Arctic (a)	288.5	maritime Arctic

The inclusion of standard deviations determines an equatorward boundary (in January  $\bar{\theta}_{e_p} + 3\sigma = 324.6^\circ$  A.) beyond which less than 1 percent of the polar fronts are expected, and a similar boundary relative to the Arctic front (in January  $\bar{\theta}_{e_a} - 3\sigma = 278.0^\circ$  A.). These two isolines are shown as dash-dotted lines.

The analysis for areas south of  $15^\circ$  N. is generally not shown as this latitude represents a reasonable geographical limit to acceptable FNWF objective analysis and is considered close to the equatorward boundary of recognizable fronts.

## 7. EXAMPLES OF FRONTAL ANALYSIS AT 850 MB.

0000 GMT JANUARY 1, 1965

The field of positive  $GG\theta$  on figure 4 (0000 GMT January 1, 1965) is both interesting and informative. There are distinct and continuous elongated zones (mostly latitudinal) extending thousands of miles in some cases and possessing orientation and wavelike features resem-

bling fronts. Along the zones there appear centers, in some cases with magnitudes in excess of  $0.35^\circ \text{C.}/(100 \text{ km.})^2$  (see North Atlantic Ocean near  $35^\circ$  N.); such values are associated with the intensely developed baroclinic regions. In addition, there are many small isolated areas of positive  $GG\theta$  with values greater than  $0.05^\circ \text{C.}/(100 \text{ km.})^2$  (see fig. 2c, vicinity of Cuba). Since such areas appear to have little synoptic-scale significance in time or space,  $GG\theta$  regions with six or fewer grid point values greater than 0.05 units and obviously not associated with a closely adjacent  $+GG\theta$  zone of greater import were omitted in transposing from the grid printout. Patterns at the lower latitudes appear to be unrealistic in number, form, and strength as a result of the combination of real frontal zones with boundary and sparse-data effects on the objective analysis.

Next note the relation of *numerical 850-mb.* and *USWB surface* fronts.<sup>5</sup> The display is typical of results on other days. The numerical 850-mb. front is generally on the cold-air side of the manually analyzed surface front, with smallest frontal-zone slopes near warm and stationary fronts. Elevation of land surfaces must be considered in an evaluation of this aspect of the figure. Verification is best where data are most plentiful—an encouraging result. In some cases where a USWB front or frontal wave exists (as near  $45^\circ$  N.,  $180^\circ$ , and  $40^\circ$  N.,  $60^\circ$  W.) but a numerical front is obviously absent there is question of the actual existence of a front in the sense of the definition given here. A significant difference between the number of numerical and hand-analyzed fronts is noted, especially over Asia and low-latitude areas. This is mainly due to lack of verifying manual analyses, premature frontolysis in sparse-data areas, and the different criteria employed to justify existence of fronts. However, the analysis of three numerical fronts along many longitudes resembles the Canadian frontal model [4].

The average difference between manual (USWB 850-mb. analysis, limited to North America, extreme northeastern Pacific, and northwestern Atlantic) and numerical frontal positions amounts to  $3.5^\circ$  latitude over the Pacific,  $1.7^\circ$  latitude over the Atlantic, and less than  $0.4^\circ$  latitude over the dense-data United States area.

Several factors detract from a "best" analysis. The processed grid-point data are too gross to single out minor or multiple frontal variations contained within a fraction of a grid distance. Besides, the data used are not "total"; the 0000 GMT operational charts generally contain about 85 percent of the practical possible amount of radiosonde data, the figure dropping to about 70 percent for the 1200 GMT maps. Analysis deadlines are, of course, necessary as the product is perishable. Amount of data must be weighed against immediate need by the field meteorologist. However, the percentage of possible data considered

<sup>4</sup> Without doubt, the transverse distance from the ridge to the zero  $GG\theta$  line (toward the cold air) is a better measure of frontal-zone half width. However, the peculiarities of, and undesirable noise near, zero  $GG\theta$  (see fig. 2c) in the relative barotropic regions and sparse data areas suggested omitting the isoline of zero  $GG\theta$  in these figures, especially since the figures presented have as prime purpose establishment of the *feasibility of locating fronts*.

<sup>5</sup> Messrs. P. E. Carlson, J. L. Galloway, and P. C. Hearing [6] of the Canadian Weather Service have compared their Central Analysis Office hand analyses of January 1, 1965 to the FNWF numerical fronts. They report "... excellent agreement with the machine-computed fronts."

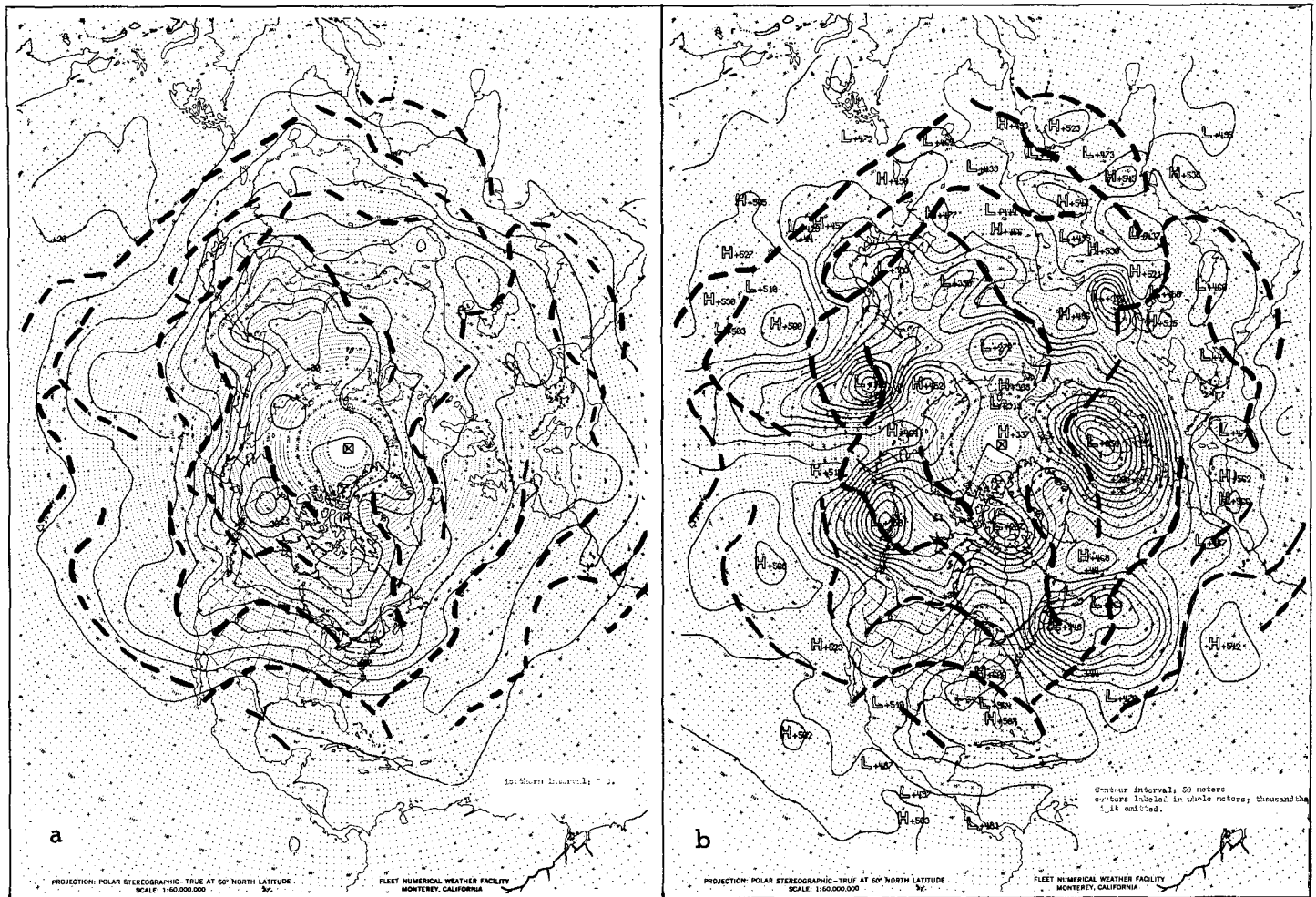


FIGURE 5.—Numerical 850-mb. fronts from figure 4 (heavy dashed lines) superimposed on the 850-mb. FNWF (a) isotherm analysis and (b) contour analysis.

for numerical analysis, say 4 hr. after observation time, easily exceeds that normally considered by an individual analyst.

Next, consider the objective frontal analysis when it is superimposed on the FNWF 850-mb. temperature (fig. 5a) and contour field (fig. 5b). The  $GG\theta$  field, of course, is just a reflection of the frontal character of the isotherm field and as such cannot exceed the information of this field. Note that in many cases the fronts lie in troughs and pass through low centers or are only slightly displaced from them. The fronts at subtropical latitudes rather remarkably pass through (or nearly so) many 850-mb. low centers, perhaps giving evidence of internal consistency in the analysis model used by FNWF. The reader will also note in this and subsequent figures that the numerical-front analysis makes little or no attempt to fit the fronts into preconceived models. However, such a procedure becomes quite suggestive when superimposing the contour and frontal patterns as in figure 5.

#### 1200 GMT JANUARY 1, 1965

Next, the 850-mb. chart for 1200 GMT January 1, 1965 is shown (fig. 6). Note the same features as in figure 4. The patterns appear more segmented over the Eastern Hemisphere. Since the data count is down for this time and the USWB surface frontal structure is more complex over the United States (frontogenesis and frontolysis over central and southern United States, respectively) the comparative result (USWB vs. FNWF) on a hemispheric basis is not as good as at 0000 GMT. Here, the differences between the FNWF and USWB 850-mb. frontal positions amount to 2.8°, 2.3°, and 1.7° for the Pacific, Atlantic, and United States areas, respectively.

#### TIME CONTINUITY, 0000 TO 1200 GMT JANUARY 1, 1965

A measure of the temporal continuity is given by the 12-hr. history chart (fig. 7). Solid lines represent the 1200 GMT January 1, 1965 fronts while dashed lines represent the 0000 GMT solutions. The USWB fronts, only

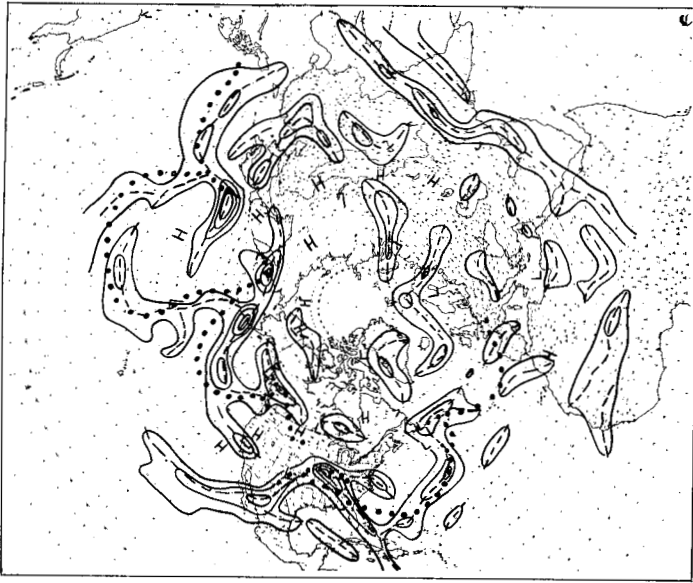


FIGURE 6.— $GG\theta$  at 850 mb. for 1200 GMT January 1, 1965; legend and units same as in figure 4.

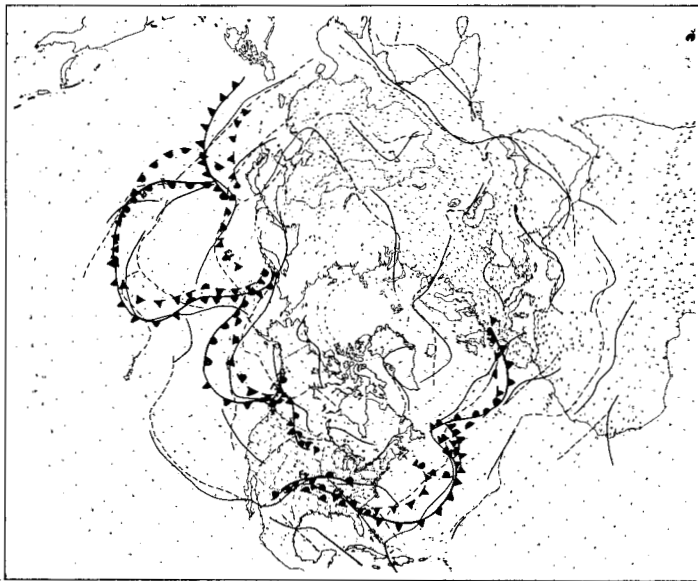


FIGURE 7.—Time continuity of numerical 850-mb. fronts January 1, 1965 (0000 GMT, dashed lines; 1200 GMT, solid lines), and U.S. Weather Bureau surface fronts shown by usual frontal symbols (0000 GMT, symbols not connected; 1200 GMT, symbols connected by line).

show the warm, cold, and stationary symbols. Similar wavelike features, developments, and movements are trackable in the hand-analyzed surface and the numerical fronts. Even over the poor-data area of Asia there is a close relation in number and orientation of numerical fronts at 0000 and 1200 GMT.

The North American and Atlantic fronts, in particular, agree well with the geostrophic movement implied by the

FNWF 850-mb. contour patterns at 0000 (fig. 5) and 1200 GMT (not shown).

## 8. EXAMPLES OF FRONTAL ANALYSIS AT THE SURFACE AND OTHER CHARTS

Space doesn't permit portrayal of all the many types of experimental charts, but two other aspects are worthy of mention. A surface frontal analysis is, of course, most desirable. Figure 8, 0000 GMT January 1, 1965, shows such a chart. Multiplicity of  $+GG\theta$  zones, in many cases small isolated regions, gives this chart an unsatisfactory segmented appearance relative to the 850-mb. depiction. There is apparent magnification of  $GG\theta$  values in areas of elevated topography, especially in the Himalayan region of Asia and over Mexico. This is understandable since the derivatives have been taken along the sloping terrain and  $\theta$  normally increases with elevation. In the case of Mexico, boundary problems add to the complexity. However, where data are best, as over the United States, verification and pattern consistency are best. For instance, the comparison between USWB and FNWF surface fronts shows an average separation of  $<0.8^\circ$  latitude for the United States,  $2.9^\circ$  latitude for the Atlantic and eastern Pacific, and  $2.6^\circ$  latitude for the western Pacific area.

The space continuity chart (fig. 9) shows considerable pattern relation between the numerical fronts at 850 mb. and the surface, particularly for those fronts which bear close relation to the USWB frontal analysis. It is not surprising to find steep or abnormal slopes where the fronts are of the cold type when the rather large distances separating grid-point data are considered. Largest discrepancies between surface and 850 mb. are found in the vicinity of elevated terrain. There is a suggestion, in the comparison of surface and 850-mb. charts, that the size of the mesh length or manner in which the data are numerically processed does not allow adequate differentiation of frontal information at levels separated by 5,000 ft. or less.

Thus, the 850-mb. portrayal presently does excel the terrain-level chart on the basis of quite limited comparisons to the USWB analysis. The variations in surface elevation and other local effects may very well necessitate a shift to a near-surface level, or to a low tropospheric thickness field in order to achieve a satisfactory "surface" frontal analysis.

The wind has been handled as a secondary frontal parameter but nevertheless is important for consideration of horizontal cyclonic shear, movement of fronts, and developmental characteristics of the frontal zone. Figure 10 shows the field of geostrophic shear at 850 mb., 0000 GMT January 1, 1965. The  $+$  symbols indicate areas of positive (cyclonic) shear of the geostrophic wind component parallel to the isentropes. In all cases the shear is less than  $4 \text{ m. sec.}^{-1} (100 \text{ km.})^{-1}$ . Most of the numerical fronts are found in positive shear areas. Cyclonic shear

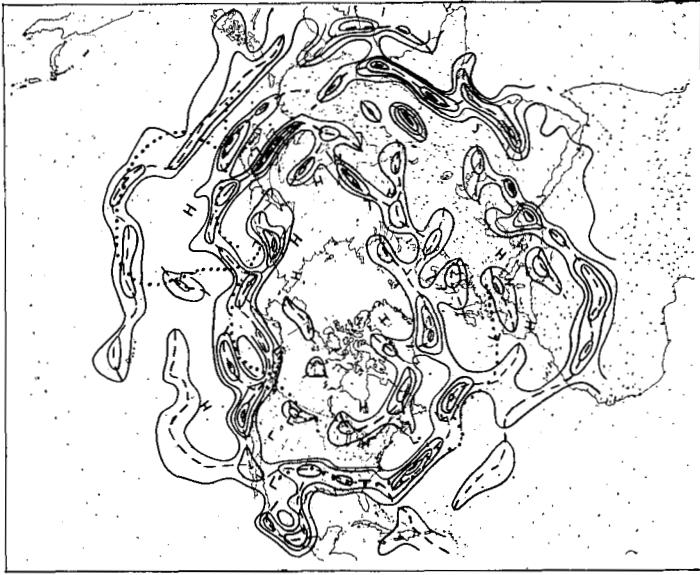


FIGURE 8.— $GG\theta$  at the surface for 0000 GMT January 1, 1965; legend and units same as in figure 4.

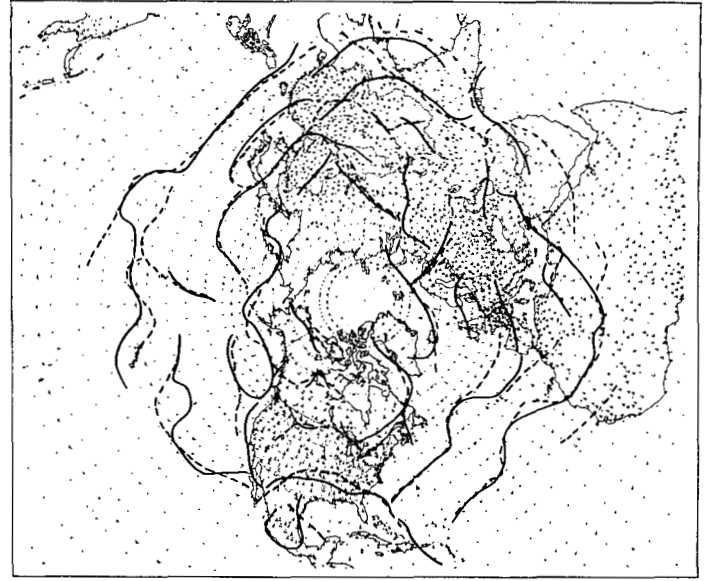


FIGURE 9.—Space continuity of numerical fronts (surface, solid lines; 850 mb., dashed lines) for 0000 GMT January 1, 1965.

tends to be at a maximum on the cold side of the front, as expected for a first-order discontinuity situation. Positive values appear especially in the area of frontal wave peaks, while anticyclonic shear appears along fronts near their most equatorward extension; the latter is not unreasonable since the narrow zones of cyclonic shear found here are difficult to portray by hand or computer analysis.

## 9. CONCLUSION

In conclusion, the authors suggest that the experimental results thus far indicate the *feasibility of hemispheric objective frontal analysis* on low-troposphere, constant-pressure surfaces. However, the ultimate goal is a three-dimensional portrayal of frontal zones at all levels. Our present and future efforts to achieve this goal include:

a. continued testing of various temperature parameters in order to obtain a frontal locator considered optimum in view of the complicating effects of terrain;

b. improving the moisture product to allow full use of  $\theta_e$  (vice  $\theta$ ) and its derivatives for frontal analysis;

c. devising a method of graphical representation similar to the present hand-produced analyses of fronts;

d. varying the mesh length of the grid; in particular, reducing its size in dense-data areas and at the surface to achieve greater detail in frontal analysis;

e. studying extensively case histories of  $GG\theta$  outputs for all seasons to allow discrimination of baroclinic zones as frontal or nonfrontal and/or those produced by spurious data and improper numerical-analysis guess fields;

f. documenting characteristics of numerical frontal patterns in relation to stages of frontal development;

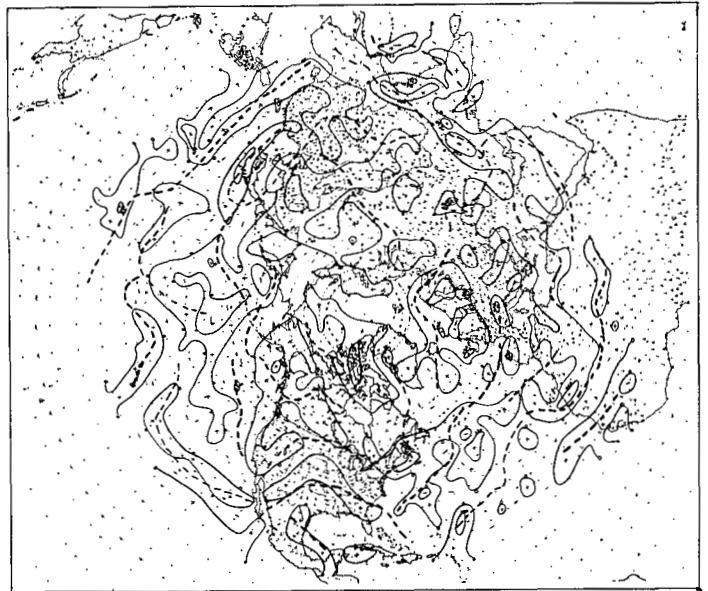


FIGURE 10.—Shear of the geostrophic wind component parallel to isentropes at 850 mb., 0000 GMT January 1, 1965. Units:  $10^{-1}$  m. sec.<sup>-1</sup> (100 km.)<sup>-1</sup>; isolines 0, +20. Cyclonic shear area indicated by plus symbols, anticyclonic shear areas by minus symbols.

g. establishing the climatology of numerical baroclinic zones with  $\theta_e$  and/or  $\theta$  fields;

h. incorporating the wind field more prominently, especially cyclonic shear, in locating fronts;

i. extending the program to higher levels (as 700 and 500 mb.);

j. placing the frontal product in proper relation to present and future numerical products for maximum real-time operational use.

Finally, it is to be noted that when time and space aspects of the analyzed thermal field are considered, the concept of a front becomes a rather restricted view of the situation. Rather one should fit this entity into a more general three-dimensional scheme of baroclinic zones.<sup>6</sup> In this sense the frontal problem becomes a subordinate problem. This broader perspective will be basic to our future experimentation and development.

#### ACKNOWLEDGMENTS

The authors wish to thank all the weather services listed under figure 1 for responding to requests for maps and various other data. The Meteorological Branch, Department of Transport, Canada, in particular, has supplied many analyses. Various members of the U.S. Navy Fleet Numerical Weather Facility and the Department of Meteorology and Oceanography, U.S. Naval Postgraduate School, Monterey, Calif., are also thanked for contributing their time and advice on matters concerning these experiments.

<sup>6</sup> This view, in fact, is in general agreement with the analysis philosophy expressed by J. S. Sawyer [7] in his 1964 Presidential Address to the Royal Meteorological Society.

#### REFERENCES

1. J. J. Taljaard, W. Schmitt, and H. van Loon, "Frontal Analysis with Application to the Southern Hemisphere," *Notos*, vol. 10, No. 1/4, 1961, pp. 25-58.
2. W. L. Godson, "Synoptic Properties of Frontal Surfaces," *Quarterly Journal of the Royal Meteorological Society*, vol. 77, No. 334, Oct. 1951, pp. 633-653.
3. M. H. Holl, J. P. Bibbo, and J. R. Clark, "Linear Transforms for State Parameter Structure," Second Ed., *Technical Memorandum No. 1*, Meteorology International, Inc., Monterey, Calif., 1963, 29 pp.
4. R. Anderson, B. W. Boville, and D. E. McClellan, "An Operational Frontal Contour-Analysis Model," *Quarterly Journal of the Royal Meteorological Society*, vol. 81, No. 350, Oct. 1955, pp. 588-599.
5. W. S. Harley, "Distributions of Wet Bulb Potential Temperature in North American Air Masses (1957) and a Statistical Analysis of Results," *Technical Circular Series*, CIR-3623 TEC-400, Meteorological Branch, Department of Transport, Canada, 1962, 46 pp.
6. P. E. Carlson, J. L. Galloway, and P. C. Hearing, "A Note on Objective Locations of Frontal Zones," *Meteorological Magazine*, vol. 94, No. 1116, July 1965.
7. J. S. Sawyer, "Meteorological Analysis—A Challenge for the Future," *Quarterly Journal of the Royal Meteorological Society*, vol. 90, No. 385, July 1964, pp. 227-247.

[Received April 20, 1965]